Tanzania Journal of Science 51(1): 65-76, 2025
ISSN 0856-1761, e-ISSN 2507-7961

Interpretation of Breakage Mechanisms in Comminution Processes by Using Particle Shape Properties: The Case Study at Buzwagi Comminution Circuit

Sospeter P. Maganga[1], Alphonce Wikedzi[2*] and Kaniki Tumba[3,4]

[1]The University of Dodoma, College of Earth Sciences and Engineering, Department of Mining and Mineral Processing Engineering, P.O. Box 11090, Dodoma, Tanzania

[2]University of Dar es Salaam, School of Mines and Geosciences, Department of Mining and Mineral Processing Engineering, P.O. Box 35131, Dar es Salaam, Tanzania

[3]Mangosuthu University of Technology, Department of Chemical Engineering, Durban, South Africa

[4]Université Officielle de Bukavu, Karhale Campus, School of Mines, Bukavu, Democratic Republic of Congo

** Corresponding author, email: alpho20012001@gmail.com*

Received 3 Mar 2024, Revised 27 Aug 2024, Accepted 5 Mar 2025, Published 14 April 2025
https://dx.doi.org/10.4314/tjs.v51i1.6

Abstract

This study interprets the breakage mechanisms at Buzwagi comminution circuit by using particle shape properties. The particle shape properties of aspect ratio, angularity, convexity and solidity were acquired from a mineral liberation analyser using DataView software. The results indicated that ground particles at Buzwagi comminution circuit were more elongated with mean aspect ratio ranges from 1.5893 to 1.6426, less angular with mean angularity values from 0.3770 to 0.4137 and smoother with mean convexity values from 0.9766 to 0.9817. The study concludes that ore particles at Buzwagi comminution circuit were ground by the combination of impact as a dominant mechanism and abrasion as a less dominant mechanism. The information on particle shape properties from comminution circuit can be used to predict the performance of downstream processes such as gravity and flotation.

Keywords: Breakage mechanism; Particle shape properties; Comminution circuit; MLA DataView; Gold ore.

Introduction

The use of particle shape properties in mineral processing design and operations is increasing nowadays due to advances in image analysis technologies such as mineral liberation analysis (MLA), scanning electron microscopy (QEMSCAN) and X-ray micro-computer tomography among others. Particle shape plays an important role in various mineral processing operations. In grinding operation, it can be used to interpret the type of breakage mechanism occurring in the comminution devices. For instance, grinding mills employing impact breakage mechanism cause bulk fracture which results in the production of irregular and elongated particles whereas mills using attrition and abrasion breakage mechanisms tend to produce more spherical and rounded particles (Pourghahramani 2012, Asghari *et al*. 2020).

Moreover, in flotation process, angular and elongated particles favor high flotation recovery and high degree of entrainment compared to rounded particles (Vizcarra *et al*. 2011b, Wiese and O'Connor 2016). In filtration process, spherical particles have lower cake resistance compared to non-spherical particles (Bourcier *et al*. 2016). In equipment wearing such as as mill liners and slurry pumps, the wearing rate decreases with an increase in particle circularity (Walker and Hambe 2015, Xu *et al*. 2019). In rheological properties such as slurry viscosity, spherical particles show lowest viscosity compared to non-spherical particles (He *et al*. 2004). In surface liberation measurements, particle shape factors such as aspect ratio has great influence on stereological bias (Ueda *et al*. 2017, Ueda *et al*. 2018).

Mineral particles are generally irregular in shapes and previous investigators have reported various particle shape parameters to describe them. This includes aspect ratio or elongation (Abazarpoor et al. 2018), angularity (Vizcarra et al. 2011a), circularity (Barani et al. 2021), roughness (Abazarpoor et al. 2018), equivalent circle diameter (Abazarpoor et al. 2018) and roundness (Little et al. 2017). The detail of common particle shape parameters is described in Table 1 using equations 1-8.

Many previous investigators (*e.g*., Frances et al. 2001, Yekeler et al. 2004, Ulusoy 2008, Verrelli et al. 2014, Little *et al.* 2015, Little et al. 2016, Abazarpoor and Halali 2017, Kinnarinen *et al*. 2017, Little *et al*. 2017, Moosakazemi et al. 2017, Abazarpoor *et al*. 2018, Ma *et al*. 2018, Yin et al. 2019, Asghari et al. 2020, Guven et al. 2020, Ulusoy 2020, Barani *et al*. 2021, Uysal *et al.* 2021) on particle shape characterization in mineral processing have studied materials other than gold ores. A recent study by Fuanya et al. (2019) investigated particle shapes on gold ores. However, their study focused on interpretation of the transport environment of placer gold from the source, rather than breakage mechanism in comminution process.

This study is aimed at interpreting the breakage mechanisms in comminution process by using particle shape properties. This is an extension study of the previous work by Wikedzi (2018) on the optimization and performance of grinding circuits at Buzwagi gold mine in Tanzania. Although the Buzwagi gold mine is at closure stage, the information in this study may help other mining operations with similar type of ore mineralogy and grade.

Table 1: Common particle shape parameters in mineral processing operations.

S/N	Particle shape descriptor	Formula	Silence features	References
1	Aspect ratio	$AR = \frac{L}{W}$ ……………………………………… (1) where AR is aspect ratio, L is the maximum ferret diameter (also known as maximum axis of fitted ellipse) and W is the minimum ferret diameter (minor axis of fitted ellipse).	A perfect round grain would have a flatness or aspect ratio of one while elongated grain would have aspect ratio of less or more than one.	Abazarpoor *et al*. (2018)
2	Angularity	$A = \frac{{P_p}^2}{4\pi A_p}$ ……………………………………….. (2) Where A is angularity, P_p is the perimeter of the particle along the maximum axis and A_p is the projected surface area of the particle.	A more angular particle has angularity more than one, a less angular particle have angularity value less than one and spherical particles have angularity value equal to one.	Vizcarra *et al*. (2011b)
3	Circularity	$C = \frac{4\pi A_p}{{P_p}^2}$ ……………………………………… (3) It is simply an inverse of angularity. where P_p is the perimeter of the particle along the maximum axis and A_p is the projected surface area of the particle.	A perfect circle has circularity of one while irregular shape has circularity less than one.	Barani *et al*. (2021)
4	Roughness	$R = \frac{A_s}{A_p}$ ……………………………………….. (4) where R is roughness, A_s is the smallest area of the circumscribed circle and A_p is the projected surface area of a particle.	A smooth surface has roughness of one while irregular particles tend to have high values of roughness.	Abazarpoor *et al*. (2018)
5	Equivalent circle diameter	$ECD = \left(\frac{4A_p}{\pi}\right)^{0.5}$ …………………………………. (5) where ECD is an equivalent circle diameter and A_p is the projected surface area of a particle.	The diameter of a circle with the same area as the particle.	Abazarpoor *et al*. (2018)

6	Roundness	$$R_o = \frac{4A_p}{\pi L^2} \quad (6)$$ where R_o is roundness of a particle, A_p is the projected surface area of a particle and L is the maximum ferret diameter.	A more round particle have roundness value approaching one.	Little *et al*. (2017)
7	Convexity	$$C_x = \frac{P_c}{P_p} \quad (7)$$ where C_x is convexity of a particle, P_c is the convex hull perimeter of the particle and P_p is the actual perimeter of the particle.	It is a measure of the particle edge roughness. As shape become smoother, convexity is approaching one.	Olson (2011a)
8	Solidity	$$S = \frac{A_p}{A_c} \quad (8)$$ where S is solidity of a particle, A_p is projected surface area of the particle and A_c is the convex hull area.	It is a measure of the overall concavity of the particle. Very smooth, rounded particles have solidity values approaching one.	Olson (2011b)

Methodology

This study used three broad (unsieved) samples (S1-6, S2-6 and S3-6) of low grade sulphide gold ore with particle size ranges from 0 to 1 mm obtained after ball milling of crushed bulk samples. The crushed bulk samples were collected from the feed conveyor of semi autogenous grinding (SAG) mill at Buzwagi gold mine in Tanzania and were prepared through staged crushing (in laboratory jaw and cone crushers) to < 5 mm followed by ball milling before conducting mineral liberation analysis.

The mineral liberation analysis was conducted by using an automated mineralogy analyser (FEI MLA 600F system) at the Department of Mineralogy, TU Bergakademie Freiberg (Germany) by the previous investigator (Wikedzi 2018). Further details on the sample collection procedure through the grinding circuit survey campaign and mineral liberation analysis are in the previous works of Wikedzi and co-authors (Wikedzi 2018, Wikedzi *et al*. 2018, Wikedzi *et al*. 2020).

This study is an extension of previous work by Wikedzi (2018) aimed at interpreting the breakage mechanism at Buzwagi comminution circuit by using particle shape properties acquired through MLA. The MLA DataView software was used to analyse the particle shape properties (aspect ratio, angularity, convexity and solidity) where data related to particle shape parameters from MLA DataView software were exported into Microsoft excel for further analysis. The exported data was processed to remove outliers by using Equations (9-14) and was presented by using normalized frequency distribution plots.

$$Q_1 = QUARTILE\ (array, 1) \tag{9}$$

$$Q_3 = QUARTILE\ (array, 3) \tag{10}$$

$$IQR = Q_3 - Q_1 \tag{11}$$

$$Lower\ bound = Q_1 - 1.5 * IQR \tag{12}$$

$$Upper\ bound = Q_3 + 1.5 * IQR \tag{13}$$

$$Outlier = OR(target\ cell < lower\ bound, target\ cell > upper\ bound) \tag{14}$$

where Q_1 is the first quartile, Q_3 is the third quartile and IQR is the interquartile range.

Results and Discussion

Aspect ratio frequency distribution for Buzwagi gold ore comminution products

Aspect ratio frequency distribution plots for Buzwagi gold ore comminution products are presented in Figure 1. It can be seen that both samples (*i.e.*, S1-6, S2-6, and S3-6) have aspect ratios of at least one and at most three which are skewed to the left with mean values of 1.6141, 1.5893, and 1.6426 for sample S1-6, S2-6 and S3-6, respectively. This implies that, in all samples the ground particles are elongated with the highest mean value observed for S3-6, followed by S1-6 and S2-6. Moreover, the results imply that impact breakage was the dominant mechanism for particles breakage at Buzwagi comminution circuit rather than attrition breakage which often produces more round particles (Vizcarra *et al*. 2011b).

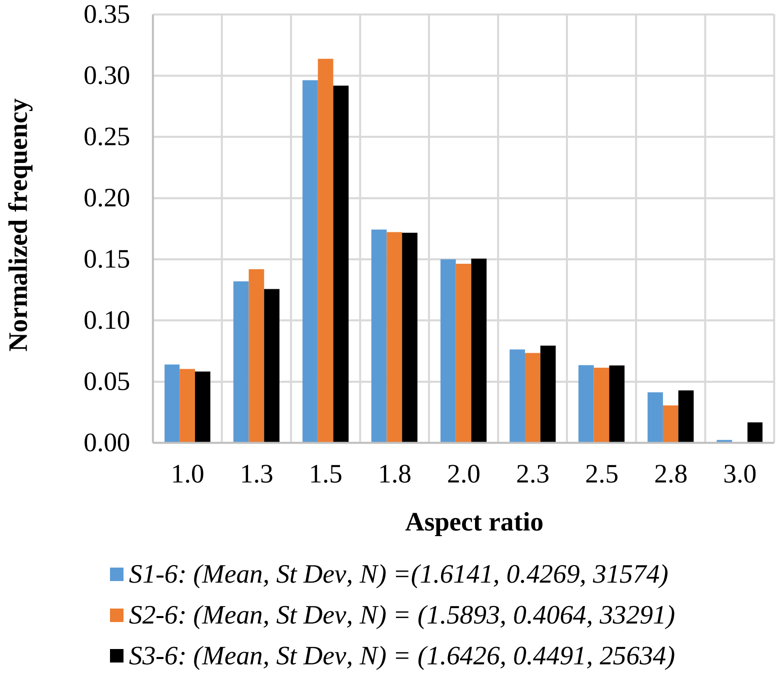

Figure 1: Aspect ratio frequency distribution plots for Buzwagi gold ore comminution products.

Angularity frequency distribution for Buzwagi gold ore comminution products

Angularity frequency distribution plots for Buzwagi gold ore comminution products are shown in Figure 2. It can be observed that particles in both samples (*i.e.*, S1-6, S2-6, and S3-6) are less angular with mean values of 0.4053, 0.3770 and 0.4137 for sample S1-6, S2-6 and S3-6, respectively, implying that particles have smoother surfaces and few edges. This information suggests that in addition to the impact breakage, there was existence of attrition forces on the particles which resulted to smooth surfaces (Vizcarra *et al*. 2011b).

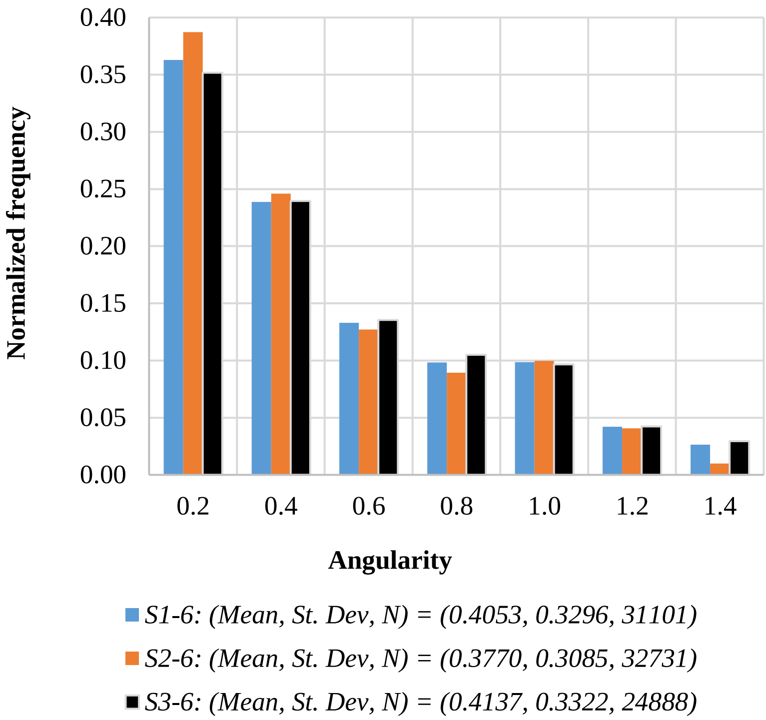

Figure 2: Angularity frequency distribution plots for Buzwagi gold ore comminution products.

Convexity frequency distribution for Buzwagi gold ore comminution products

Convexity frequency distribution plots for Buzwagi gold ore comminution products are presented in Figure 3. It can be seen that particles in all samples (*i.e.*, S1-6, S2-6, and S3-6) are smooth with mean values of 0.9790, 0.9817 and 0.9766 for sample S1-6, S2-6 and S3-6, respectively, implying that particles were smoother and there was existence of abrasion forces during the comminution process.

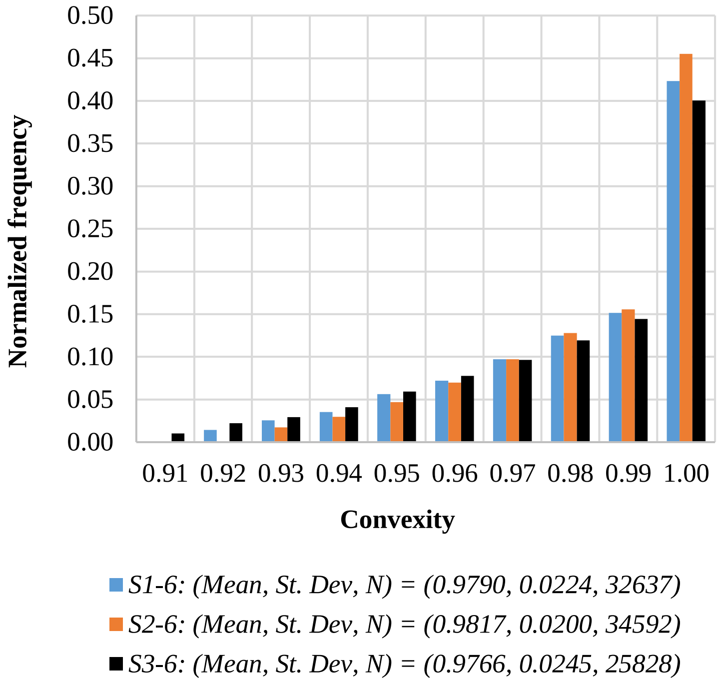

Figure 3: Convexity frequency distribution plots for Buzwagi gold ore comminution products.

Solidity frequency distribution for Buzwagi gold ore comminution products

Solidity frequency distribution plots for Buzwagi gold ore comminution products are shown in Figure 4. It can be seen that particles in all samples (*i.e.*, S1-6, S2-6, and S3-6) are smooth with mean values of 0.7240, 0.7255 and 0.7315 for sample S1-6, S2-6 and S3-6, respectively. These results correlate with those observed from Figure 2 and Figure 3, implying the existence of abrasion forces during comminution processes.

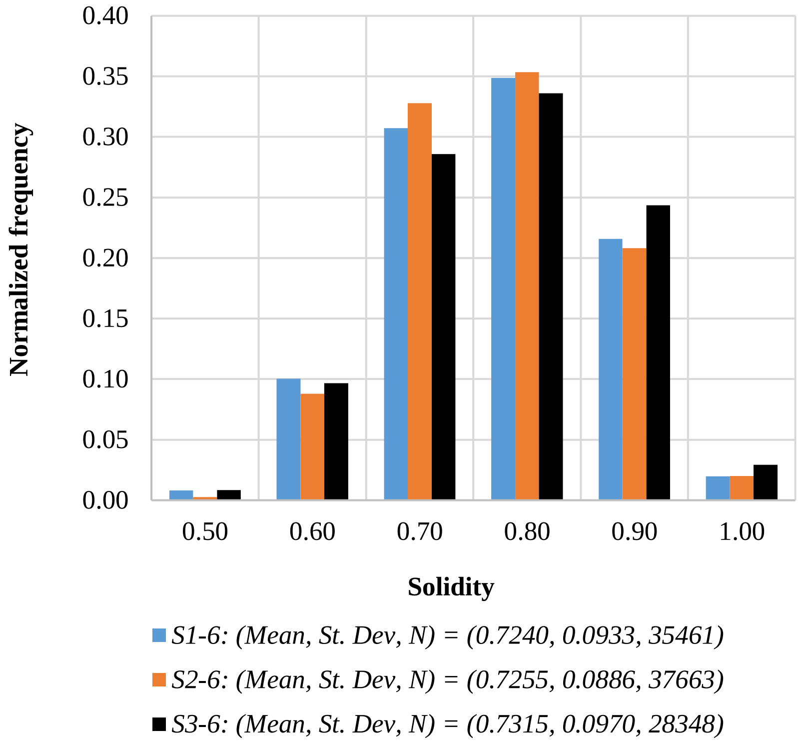

Figure 4: Solidity frequency distribution plots for Buzwagi ore comminution products.

Particle shape images of Buzwagi gold mine comminution products

The particle shape images for Buzwagi comminution products are shown in Figure 5. It can be seen that all samples (S1-6, S2-6 and S3-6) products are elongated and have smooth surfaces. This implies the presence of both impact and abrasion forces during the comminution process. Moreover, the main gold bearing mineral phase (pyrite-pyrrhotite) has more smooth surfaces compared to many gangue minerals. Therefore, particle shape images provide qualitative information on the type of breakage mechanisms involved during the comminution process.

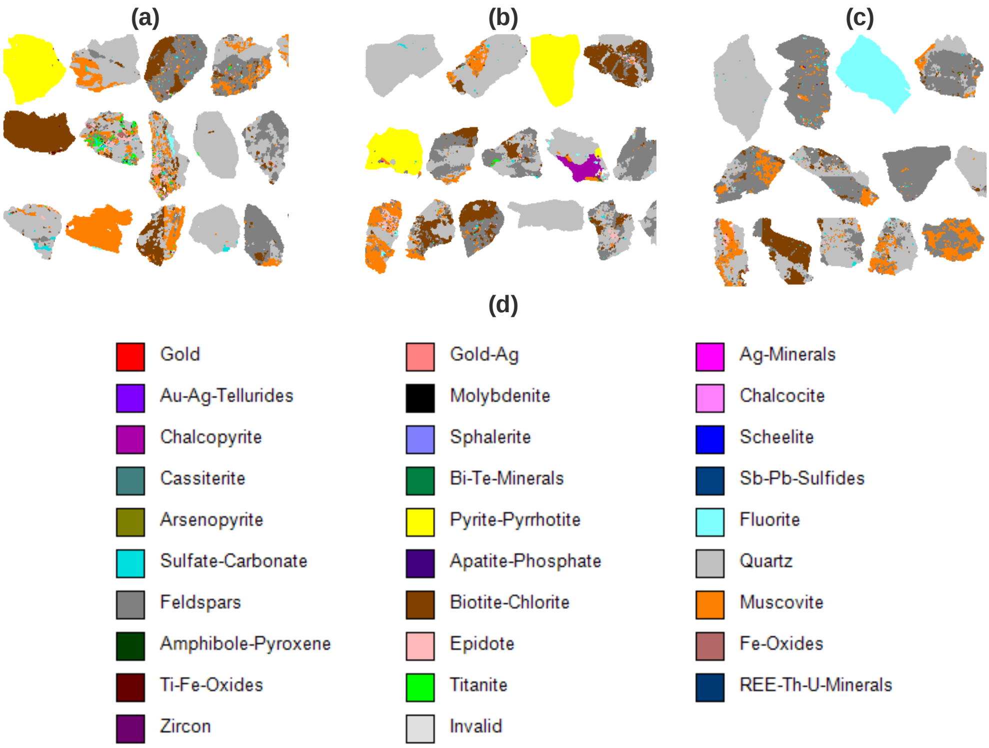

Figure 5: MLA particle shape images for Buzwagi ore comminution products: (a) Sample S1-6, (b) Sample S2-6, (c) Sample S3-6 and (d) Legend.

Conclusions

The interpretation of breakage mechanisms of Buzwagi comminution circuit by using particle shape properties was conducted and concluded that ground particles at Buzwagi comminution circuit are more elongated with mean aspect ratio ranges from 1.5893 to 1.6426, less angular with mean angularity values from 0.3770 to 0.4137 and smoother with mean convexity values from 0.9766 to 0.9817. This implies ore particles at Buzwagi comminution circuit were ground by the combination of impact as a dominant mechanism and abrasion as less dominant mechanism. In addition, the information of particle shape properties of ground particles can be used to forecast the performance of downstream mineral processes such as gravity and flotation.

Acknowledgements

The authors would like to thank the Buzwagi Gold Mine for provision of the ore material and the Department of Mineralogy, TU Bergakademie Freiberg (Germany) for mineral liberation analysis.

References

Abazarpoor A and Halali M 2017 Investigation on the particle size and shape of iron ore pellet feed using ball mill and HPGR grinding methods. *Physicochem. Proble. Miner. Process.* 53: 908-919.

Abazarpoor A, Halali M, Hejazi R and Saghaeian M 2018 HPGR effect on the particle size and shape of iron ore pellet feed using response surface methodology. *Miner. Process. Extr. Metall.* 127: 40-48.

Asghari M, VandGhorbany O and Nakhaei F 2020 Relationship among operational parameters, ore characteristics, and product shape properties in an industrial SAG mill. *Part. Sci. Technol.* 38: 482-493.

Barani K, Azadi MR and Moradpouri F 2021 Microwave Pretreatment on copper sulfide ore: comparison of ball mill grinding and bed breakage mechanism. *Min. Metall. Explor.* 38: 2209-2216.

Bourcier D, Féraud JP, Colson D, Mandrick K, Ode D, Brackx E and Puel F 2016 Influence of particle size and shape properties on cake resistance and compressibility during pressure filtration. *Chem. Eng. Sci.* 144: 176-187.

Frances C, Le Bolay N, Belaroui K and Pons MN 2001 Particle morphology of ground gibbsite in different grinding environments. *Int. J. Miner. Process.* 61: 41-56.

Fuanya C, Bolarinwa AT, Kankeu B, Yongue RF, Ngatcha RB and Tangko TE 2019 Morphological and chemical assessment of alluvial gold grains from Ako'ozam and Njabilobe, southwestern Cameroon. *J. Afr. Earth Sci.* 154: 111-119.

Guven O, Serdengecti MT, Tunc B, Ozdemir O, Karaagaclioglu IE and Çelik MS 2020 Effect of particle shape properties on selective separation of chromite from serpentine by flotation. *Physicochem. Proble. Miner. Process.* 56: 818-828.

He M, Wang Y and Forssberg E 2004 Slurry rheology in wet ultrafine grinding of industrial minerals: a review. *Powder Technol.* 147: 94-112.

Kinnarinen T, Tuunila R and Häkkinen A 2017 Reduction of the width of particle size distribution to improve pressure filtration properties of slurries. *Miner. Eng.* 102: 68-74.

Little L, Becker M, Wiese J and Mainza AN 2015 Auto-SEM particle shape characterisation: Investigating fine grinding of UG2 ore. *Miner. Eng.* 82: 92-100.

Little L, Mainza AN, Becker M and Wiese J 2017 Fine grinding: How mill type affects particle shape characteristics and mineral liberation. *Miner. Eng.* 111: 148-157.

Little L, Mainza AN, Becker M and Wiese JG 2016 Using mineralogical and particle shape analysis to investigate enhanced mineral liberation through phase boundary fracture. *Powder Technol.* 301: 794-804.

Ma G, Xia W and Xie G 2018 Effect of particle shape on the flotation kinetics of fine coking coal. *J. Clean. Prod.* 195: 470-475.

Moosakazemi F, Mohammadi MT, Mohseni M, Karamoozian M and Zakeri M 2017 Effect of design and operational parameters on particle morphology in ball mills. *Int. J. Miner. Process.,* 165: 41-49.

Olson E 2011a Particle shape factors and their use in image analysis–part 1: theory. *J. GXP Compliance.* 15: 85-96.

Olson E 2011b Particle shape factors and their use in image analysis part II: practical applications. *J. GXP Compliance.* 15: 77.

Pourghahramani P 2012 Effects of ore characteristics on product shape properties and breakage mechanisms in industrial SAG mills. *Miner. Eng.* 32: 30-37.

Ueda T, Oki T and Koyanaka S 2017 Effect of particle shape on the stereological bias of the degree of liberation of biphase particle systems. *Mater. Trans.* 58: 280-286.

Ueda T, Oki T and Koyanaka S 2018 Numerical analysis of the general characteristics of stereological bias in surface liberation assessment of ore particles. *Adv. Powder Technol.* 29: 3327-3335.

Ulusoy U 2008 Application of ANOVA to image analysis results of talc particles produced by different milling. *Powder Technol.* 188: 133-138.

Ulusoy U 2020 Comparison of particle shapes of conventionally ground barite, calcite and talc minerals by dynamic imaging technique: A review. *EUREKA: Phys. Eng.* 5: 80-90.

Uysal T, Guven O, Ozdemir O, Karaagaclioglu IE, Tunç B and Çelik MS 2021 Contribution of particle morphology on flotation and aggregation of sphalerite particles. *Miner. Eng.* 165: 106860.

Verrelli DI, Bruckard WJ, Koh PT, Schwarz MP and Follink B 2014 Particle shape effects in flotation. Part 1: Microscale experimental observations. *Miner. Eng.* 58: 80-89.

Vizcarra TG, Harmer SL, Wightman EM, Johnson NW and Manlapig EV 2011a The influence of particle shape properties and associated surface chemistry on the flotation kinetics of chalcopyrite. *Miner. Eng.* 24: 807-816.

Vizcarra TG, Wightman EM, Johnson NW and Manlapig EV 2011b. The effect of breakage method on the shape properties of an iron-oxide hosted copper–gold ore. *Miner. Eng.* 24: 1454-1458.

Walker CI and Hambe M 2015 Influence of particle shape on slurry wear of white iron. *Wear* 332: 1021-1027.

Wiese JG and O'Connor CT 2016 An investigation into the relative role of particle size, particle shape and froth behaviour on the entrainment of chromite. *Int. J. Miner. Process.* 156: 127-133.

Wikedzi A 2018 *Optimization and Performance of Grinding Circuits: The case of Buzwagi Gold Mine (BGM).* PhD Thesis, Technische Universität Bergakademie Freiberg.

Wikedzi A, Arinanda MA, Leißner T, Peuker UA and Mütze T 2018 Breakage and liberation characteristics of low grade sulphide gold ore blends. *Miner. Eng.* 115: 33-40.

Wikedzi A, Saqurana S, Leißner T, Peuker UA and Mütze T 2020 Breakage characterization of gold ore components. *Miner. Eng.* 151: 106314.

Xu L, Luo K, Zhao Y, Fan J and Cen K 2019 Influence of particle shape on liner wear in tumbling mills: A DEM study. *Powder Technol.* 350: 26-35.

Yekeler ME, Ulusoy, UĞ and Hiçyılmaz C 2004 Effect of particle shape and roughness of talc mineral ground by different mills on the wettability and floatability. *Powder Technol.* 140: 68-78.

Yin W, Zhu Z, Yang B, Fu Y and Yao J 2019 Contribution of particle shape and surface roughness on the flotation behavior of low-ash coking coal. *Energy Sources A: Recovery Util. Environ. Eff.* 41: 636-644.